Plasmodial vein networks of the slime mold *Physarum polycephalum* form regular graphs

Werner Baumgarten,[1] Tetsuo Ueda,[2] and Marcus J. B. Hauser[1,*]
[1]*Institut für Experimentelle Physik, Abteilung Biophysik, Otto-von-Guericke Universität Magdeburg, Universitätsplatz 2, 39106 Magdeburg, Germany*
[2]*Research Institute for Electronic Science, Hokkaido University, N-20 W-10, Sapporo 001-0020, Japan*
(Received 17 June 2010; published 22 October 2010)

The morphology of a typical developing biological transportation network, the vein network of the plasmodium of the myxomycete *Physarum polycephalum* is analyzed during its free extension. The network forms a classical, regular graph, and has exclusively nodes of degree 3. This contrasts to most real-world transportation networks which show small-world or scale-free properties. The complexity of the vein network arises from the weighting of the lengths, widths, and areas of the vein segments. The lengths and areas follow exponential distributions, while the widths are distributed log-normally. These functional dependencies are robust during the entire evolution of the network, even though the exponents change with time due to the coarsening of the vein network.

DOI: 10.1103/PhysRevE.82.046113 PACS number(s): 05.65.+b, 87.17.Pq, 89.75.Fb, 89.75.Hc

I. INTRODUCTION

Transportation networks are ubiquitous in both biological and technical systems. A problem of the topology of transportation networks, namely, the problem of the bridges of Königsberg, has lead to the foundation of graph theory. Since then, graph theory has been developed and applied to solve a multitude of problems, including transportation networks [1]. However, in the last decades, an increasing number of evolving transportation networks was found not to behave according to the rules of the classical graph theory, but to possess features that are typical for complex dynamic networks. Since in the real world evolving transportation networks following the classical graph theory are seldom, graph theory has been extended to complex network theory [2] by introducing new classes of graphs, such as random [3] and small-world graphs [2,4].

One important property of networks is their topology, i.e., the connectivity pattern of the nodes of a network or graph. Small-world networks lie between completely regular and completely random graphs [4], and are characterized by the occurrence of connections between distinctively different regions separated from each other by large distances in the network. Many of these networks are scale-free, i.e., they show a power-law degree distribution [2]. Networks in the real world also very frequently possess some highly connected nodes that act as hubs. Examples can be found among man-made and biological transportation networks, such as the air transportation [5,6] and railway networks [7,8], electric power grids [4], as well as in blood vascularization networks [9] and insect trails and galleries [10,11]. Small-world networks are also abundant in social and economic activities, as shown for scientific co-author [12] or co-starring film actors networks [4], and the world trade network [13]. For an overview see Refs. [2,3].

The second important property defining any network is the weight or intensity associated with each of the connections (edges) between a connected pair of nodes. Together, the topology and the weighting of the connections determine the performance and dynamics of a network [2]. Real-world networks generally display a large heterogeneity in the weights of the connections.

Which topological network structure optimizes a network with respect to a given transportation characteristics is an important topic of current research [14,15]. The optimal topology depends strongly on the optimizing functional, i.e., the functional task with respect to which the network was optimized. For instance, networks optimized for high throughput efficiency form topological trees without any loops [14,16]. This means that the rupture of an edge leads to two disconnected sub-networks. By contrast, networks optimized with respect to resilience to damage will contain loops, since they provide alternative pathways through the network once an edge is removed or ruptured [17,18]. Recently, loop-containing networks were also identified as optimal for handling a spatially and temporally varying transportation load [17].

In the present article, we analyze the structure of the transportation vein network of the plasmodium of the slime mold (myxomycete) *Physarum polycephalum* [19]. The plasmodium is a multinucleate giant single cell that moves about with amoeboid motility. Its large aggregate of protoplasm extends over some tens of square centimeters and forms a vein network, through which its protoplasm flows to and fro periodically due to differences in hydrostatic pressure [20]. Thus, geometric parameters such as the lengths and widths of the veins are related quantitatively to the performance of the edges between the nodes.

Moreover, the plasmodium is able to adapt to the environmental conditions by changing its shape dynamically, notably by optimizing the structure of its vein network [21–23]. In the presence of multiple food sources, the cell connects them through its vein network at a minimum cost. This is achieved by shrinking all veins other than those providing the direct connection between the food sources. This property has been exploited to let the slime mold solve a maze [24,25] or other graph theoretical problems, like constructing Steiner minimum pathway trees [26], or finding minimum-

*Corresponding author. FAX: +49–391–6711181; marcus.hauser@ovgu.de

risk pathways in an environment, where the slime mold is subjected to two competing cost factors [27]. In fact, it has recently been shown that the optimization of the plasmodial vein network aims at simultaneously reducing the network length, increasing the transport efficiency in the vein system, and achieving a high fault tolerance of the network against rupture of individual veins [23].

Surprisingly, the graph properties of the plasmodial vein network have not been investigated yet. In earlier papers the vein network is described colloquially as a more or less regular network [28], and recently it was assumed that the network possesses a narrow node degree distribution [29].

In the present paper, we wish to unravel the topological structure and the weighting pattern realized in the plasmodial vein network of *P. polycephalum*. To this purpose images of the expanding plasmodial network are acquired and subsequently analyzed. It is found from the connectivity of the nodes in the plasmodium that this slime mold forms regular graphs in the sense of graph theory. Finally, we determine the statistical properties of the vein segments connecting every pair of nodes, and follow their development as the vein network becomes larger and larger with time.

II. MATERIALS AND METHODS

The plasmodia of the slime mold *Physarum polycephalum*, strain HU195×HU200 [30], were cultured on moist filter paper by feeding with oat flakes (Kölln Flocken) at 21 °C in the dark. Sclerotia were obtained by drying the wet filter paper on which a sufficient amount of the plasmodium had crawled, and stored in the dark for 3 to 10 months. The sclerotium is a dormant, dehydrated state of *P. polycephalum* that may convert back into the plasmodium whence the environmental conditions turn favorable again.

For experiments, 1% (w/v) plain agar gels (Difco BactoAgar) were prepared in square polystyrene Petri dishes (10×10 cm^2). A strip of filter paper (70×5 mm^2) covered with sclerotia was moistened and placed on the agar gel along one edge of the dish. The sclerotia germinated and the plasmodium began to expand over the agar gel after about 26 000 s. This evolving plasmodium expanded over the gel layer and began to form a network of veins and venules (Fig. 1). Since the network formation was sensitive to humidity and temperature, the Petri dish was covered and the temperature kept constant at 21.0±0.5 °C.

The Petri dish was illuminated homogeneously from below by a cold light source (Polytec) emitting white light and monitored from above by an 8 bit charge controlled device (CCD) camera (Hamamatsu C3077). The images were collected with a resolution of 768×576 pix^2 corresponding to an area of 61.5×46.1 mm^2 (i.e., a resolution of 0.08 mm pix^{-1}) at a sampling frequency of 0.1 Hz. The frames were transferred to a computer for later data processing and analysis. This analysis involves the extraction of the vein network from the acquired images. To this purpose, the background-subtracted images were binarized, corrected for missing pixels, and finally collapsed to their skeletonized graphs, as reported in detail in Ref. [31]. In the skeletonized images, the nodes were defined as the branching points of the

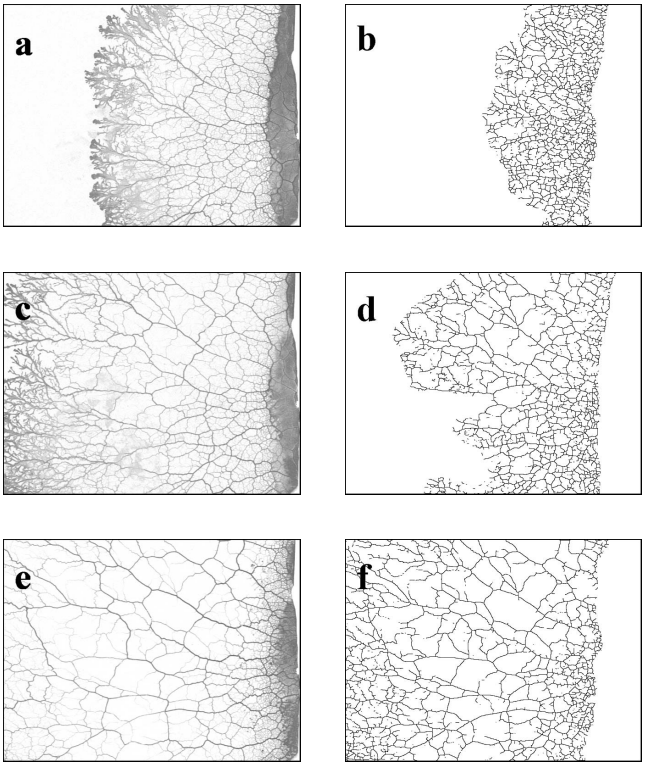

FIG. 1. Development of the plasmodial vein network of *Physarum polycephalum*. The left column shows the background-subtracted images at (a) $t=54\,000$ s, (c) $t=60\,000$ s, and (e) $t=70\,000$ s, while the right column shows the corresponding skeletonized regions of the networks ((b) $t=54\,000$ s, (d) $t=60\,000$ s, and (f) $t=70\,000$ s). The plasmodium begins to grow from the right edge of the frames at $t\sim 26\,000$ s after the start of the experiment. The area of observation is always 61.5×46.1 mm^2.

venes. A vene connecting a pair of nodes was defined as an edge of the graph. Since in between two nodes there were no subdivisions, a long vein was considered as a single edge [31]. These procedures were repeated for all images, giving access to the temporal evolution of the graph.

The binarization of images requires the selection of a threshold value. To obtain a robust extracted graph, the images were binarized using a series of threshold values that vary slightly around the optimal binarization threshold [31] and subsequently corrected and collapsed to the skeletonized graphs. Those domains of the skeletonized networks that were not affected by the small variations in the threshold value for the binarization, were used for the analysis of the network structure [see Figs. 1(b), 1(d), and 1(f)]. The surface covered by such a domain is the area A of the region of investigation.

III. RESULTS

The plasmodium of *Physarum polycephalum* strain HU195×HU200 exhibits a peculiar shape, which is characteristic for myxomycetes. Figure 1 depicts the background-subtracted images of the plasmodium, as well as the corresponding skeletonized graphs [the domains shown in Figs.

1(b), 1(d), and 1(f) are the domains A of the skeleton that can be extracted unambiguously]. The protoplasm distributes densely near the extending front, and in the wake of this apical zone the plasmodium transforms into a complex network of tubular veins, in which protoplasm flows vigorously to and fro. Thus, the vein system ensures that the large plasmodium behaves as a single organism. As the plasmodium advances, the vein network becomes sparser.

The organization of the plamsodial vein network was analyzed in the context of graph theory. Each branching point of the network forms a node that is connected to other nodes via veins or venules. The latter form the edges of the graph **G**, which is given by

$$\mathbf{G} = \mathbf{F} \cdot \mathbf{A}, \tag{1}$$

where **A** is the adjacency matrix that denotes whether a pair of nodes is connected, while the matrix **F** contains the areas of the vein segments (edges). The adjacency matrix **A** defines the topology of the graph, while **F** encodes the weights of the connections (or edges).

A. Topology of the vein network

The topology of the plasmodial vein networks is given by the adjacency matrix **A**, which is extracted from the experimental data by identifying all pairs of connected nodes present in the skeletonized graphs. Connected nodes lead to entries $a_{ij}=1$ in the adjacency matrix **A**, unconnected nodes to entries $a_{ij}=0$. The number of connections leaving (or entering) each node is also determined; this corresponds to a row-wise summation over the entries $k=\Sigma_j a_{ij}$ of matrix **A**. Each individual node is found to be connected to exactly three other nodes. This property is preserved during the entire evolution of the vein network. The connectivity of a node is its node degree k. Graphs with delta distributed node degrees are called regular and they are characterized by a constant ratio of edges to nodes

$$M = \frac{1}{2}kN, \tag{2}$$

where M and N are the number of edges (veins) and nodes, respectively. This correlation is indeed fulfilled in the studied vein network (Fig. 2), where the ratio of edges to nodes is 1.56 ± 0.06. Thus, in terms of graph theory, the vein network of *P. polycephalum* forms a regular graph of degree 3, also known as a cubic graph.

The clustering coefficient c of the vein network measures to which extent the neighboring edges of a given edge are connected among each other. Hence the clustering coefficient c provides an indication for how close the graph is to form a clique (where any member knows all other members of the clique, therefore $c=1$) [4]. In the *P. polycephalum* vein network we obtained $c=0.021 \pm 0.005$. This relatively low value is consistent with the regular graph nature of the plasmodial vein network. As the network expands, the value of c decreases.

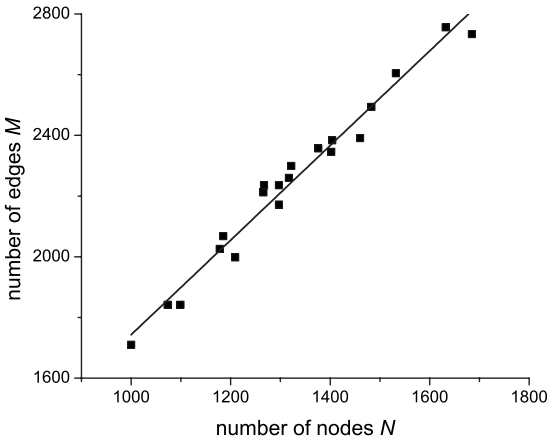

FIG. 2. Dependence of the number of veins (edges) M from the number of nodes N. The number of edges increases 1.56 ± 0.06 times faster than the number of nodes.

B. Weights of the edges

In real-world networks the connections between the nodes (i.e., the edges) frequently possess nonuniform weights. Such networks are called weighted networks. In fact, the plasmodial vein network also displays heterogeneities in the intensity of the vein connections. Therefore, we determine the lengths of the veins (compiled in matrix **L**), their widths (matrix **W**), and their areas [matrix **F**, Eq. (1)]. The ij-th entry of the matrix **F** of the areas of the veins is given by the product $\mathbf{F}_{ij}=\mathbf{W}_{ij} \cdot \mathbf{L}_{ij}$.

The distribution of the lengths of the veins between connected nodes is determined at different instants of the network development, and is found to follow the exponential dependence

$$P(x) = P_0 e^{-\gamma x}, \tag{3}$$

where $P(x)$ is the probability to find a segment of length x in the network (Fig. 3).

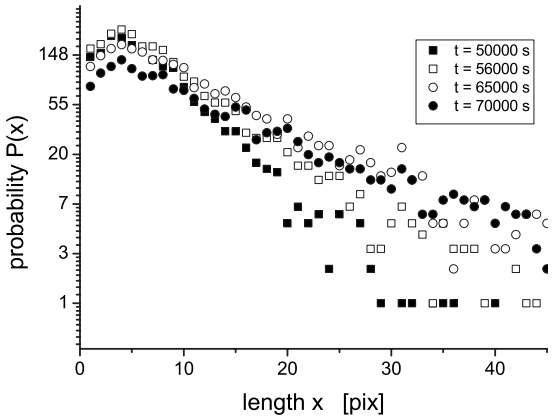

FIG. 3. Exponential scaling of the length distribution of vein segments. With time ($t=50\,000$ s, full squares; $t=56\,000$ s, open squares; $t=65\,000$ open circles; $t=70\,000$ s full circles) the slope γ of the logarithmic plots decreases, while the functional dependence still holds.

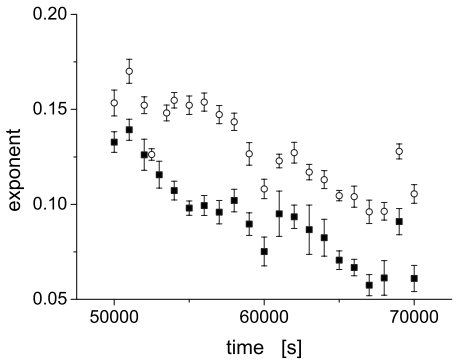

FIG. 4. Temporal evolution of the exponents γ (open circles) and α (solid squares) of the exponential probability distributions of the lengths [Eq. (3)] and areas [Eq. (7)] of the vein segments, respectively.

At early instants of the development, the expanding plasmodial vein network forms a dense mesh of short-range filaments [Figs. 1(a) and 1(b)]. With time, the network expands and its apical zone advances, exploring new spaces. At a certain distance from the apical zone, the mesh network coarsens [Figs. 1(c)–1(f)]. While the length dependence [Eq. (3)] always remains exponential, the value of the exponent γ decreases as the plasmodial vein network expands (Fig. 4). This reflects the coarsening of the tubular vein network, where tiny venules are deleted as the network evolves. As a venule disappears, so does the node associated to it. In consequence, this leads to a coarsening of the network. At the same time larger vein segments become more frequent at the expense of shorter ones, thus yielding a decreasing exponent γ.

The temporal development of the vein network is also reflected by the ratio R

$$R = \frac{\sum_i x_i}{A} \tag{4}$$

of the sum over the lengths x_i of all veins to the area A covered by the network (Fig. 5). When a plasmodium begins exploring its surroundings (i.e., from $t=50\,000$ s to $t=52\,400$ s in the experiment shown in Fig. 1), it forms a very dense vein network that searches the area for food sources. This is reflected by a high ratio R. As the apical zone advances in space, the network left behind begins to coarsen by deleting 'superfluous' tiny venules. Hence, there is a competition between the formation of a dense mesh adjacent to the apical zone and the sparsening of the vein network further away from the growth zone of the plasmodium. As the network increases, the coarsening becomes more effective, thus leading to a decrease of R (for $52\,500\ \text{s} < t < 61\,000$ s, Fig. 5). In extended plasmodia, far from the apical zone, the coarsening process approaches a limit, forming networks whose total vein length to area ratio R settles onto a stationary value of $R \sim 0.06\ \text{pix}^{-1}$. This indicates the existence of a preferred asymptotic mesh size.

Next, we focus on the matrix $\mathbf{W}$ of the widths of veins and venules. At early instants of network development, the

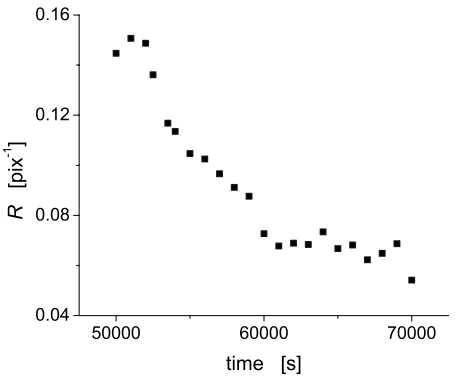

FIG. 5. Development of the ratio R of the total length of the vein network to the area covered by the plasmodium in time. "Young" networks are relatively dense, while the value of R decreases with time due to coarsening. For longer times, R approaches a constant asymptotic value.

widths of veins obey a log-normal distribution (Fig. 6), where $P(y)$ is the probability to find a vein or venule of width y. This probability scales as

$$P(y) = \frac{1}{\sigma y\sqrt{2\pi}} e^{-(1/2)(\ln y - \mu)^2/\sigma^2} \tag{5}$$

where μ is the maximum of the distribution and σ its variance. As the network coarsens, the log-normal distribution of the widths of the veins converges to a normal (Gaussian) distribution,

$$P(y) = \frac{1}{\sigma\sqrt{2\pi}} e^{-(1/2)(y - \mu)^2/\sigma^2} \tag{6}$$

whose maximum is shifted toward larger widths, reflecting the fact that in the sparse network smaller and thinner segments (venules) give way to fewer but thicker veins (Fig. 6). It should be noted that for coarsened networks the vein widths satisfy a Gaussian distribution slightly better than a log-normal one. In other words, it is also possible to fit the width distribution solely by a log-normal function.

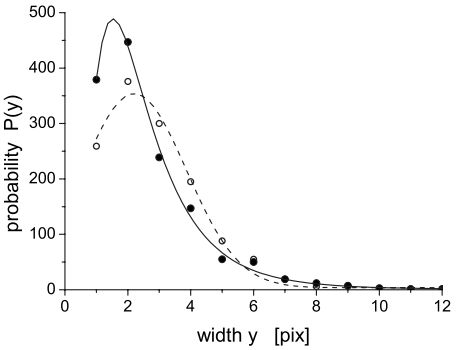

FIG. 6. Distribution of the widths y of the veins. At early stages of the plasmodial development, the widths follow a log-normal distribution ($t=56\,000$ s, solid symbols, solid line), while the width distribution becomes normal as the network coarsens ($t=68\,000$ s, open symbols, dashed line).

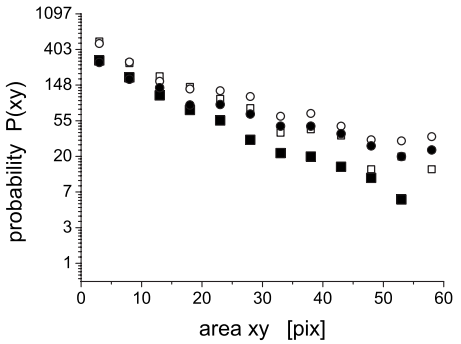

FIG. 7. Exponential scaling of the area distribution of vein segments. With time (t=50 000 s, full squares; t=56 000 s, open squares; t=65 000 open circles; t=70 000 s full circles) the slope α of the logarithmic plots decreases, while the functional dependence remains robust.

Finally, we studied the areas xy of the individual vein segments in the network. As in the case of the length distribution $P(x)$, the distribution of the areas $P(xy)$ of the veins follows an exponential distribution

$$P(xy) = P_0 e^{-\alpha xy} \tag{7}$$

as shown in Fig. 7. Again, the form of the probability distribution of the area of the veins remains exponential at all times, while the exponent α decreases as the vein network evolves (Fig. 4).

Analogously to the temporal evolution of the total length of the vein network [reflected by the ratio R defined by Eq. (4)], we have followed the evolution of the total area of the veins in time. We define the ratio S

$$S = \frac{\sum_i (xy)_i}{A} \tag{8}$$

of the total area of the veins $(xy)_i$ to the area A covered by the network. The ratio S decreases as the vein network becomes sparser (Fig. 8). In extended plasmodia the fraction of the area of the network actually covered by the veins converges to a stationary value of $S \sim 0.20$. This means that in the sparse network the plasmodium occupies about 20% of the total area spanned by the tubular vein network.

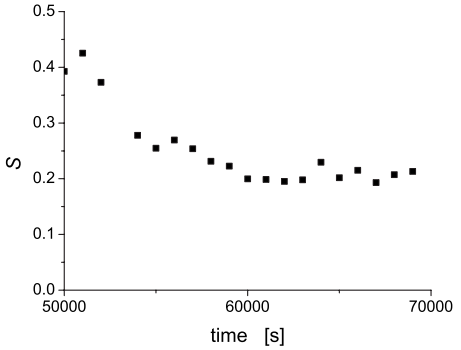

FIG. 8. Temporal evolution of the ratio S of the total area of the vein network to the area covered by the plasmodium. At early instants of plasmodial development, the network shows a high surface coverage by plasmodial cell mass. As the network becomes sparser, S decreases until it reaches an asymptotic value.

IV. DISCUSSION

The plasmodial vein network of *Physarum polycephalum* forms a regular, cubic graph. It is amazing that an extended cellular system that lacks any central controlling unit is able to reliably form a classical, regular graph, which often is considered as a somewhat artificial mathematical construct [3]. However, evolution has selected exactly this regular graph structure to very efficiently perform vital and often conflicting tasks, such as the simultaneous reduction of costs, the maximization of transport efficiency through the network, and the minimization of risks, as reported in Ref. [23].

The formation and evolution of a classical graph represents a fundamental difference to the organization of most of the evolving transport networks. For instance, the grid of power lines shows small-world characteristics [4], while the world air-transportation network is a small-world graph with scale-free properties [5,6]. Neither of these properties is found in the vein network of *P. polycephalum*.

The cubic graph nature of the plasmodial vein network is also evidenced by a ratio of 1.56 ± 0.06 edges to nodes (Fig. 2). This is slightly higher than the theoretical value of 1.5 that is obtained for infinitively large regular graphs of degree k=3. The deviation from the theoretical value is due to the coarsening of the network, which leads to the rupture of a vein into two disconnected venules. Consequently, this leads to a slightly higher ratio of edges to nodes.

The regular graph of the plasmodial vein network of *P. polycephalum* is weighted by the lengths, widths, and areas of the vein segments. Each of these three weighting matrices shows a pronounced probability distribution. While the probability to find a certain width of a vein was found to follow a log-normal or normal distribution, the lengths and the areas of the vein segments show exponential distributions. Interestingly, these functional dependencies are robust and remain valid during the entire evolution of the vein network, while the individual exponents change as the network evolves and coarsens.

The remarkable robustness of the statistical properties of the lengths, widths, and areas of the vein segments may be used to distinguish and classify different network structures and morphologies realized in different strains and mutants of *P. polycephalum* as well as in other classes of myxomycetes. Such an approach provides hard and unambiguous criteria based on statistical physics for the distinction among different network morphologies. This may help to define and discriminate between different phenotypes based on plasmodial morphology, which so far rely on colloquial descriptions of the network topology.

V. CONCLUSION

In conclusion, the vein network of *Physarum polycephalum* is one of the rare evolving transportation network systems to spontaneously form a classical regular graph which consequently does not possess small-world or scale-free

properties. Instead, all nodes have a unique degree, namely, $k=3$. This graph is weighted by the strengths of the veins connecting any pair of nodes. It is found that the lengths and areas of the segments follow distinct distributions. Although the vein network coarsens with time, the functional relations remain unaffected by the dynamics.

ACKNOWLEDGMENTS

We would like to thank the Alexander-von-Humboldt Foundation for a stipend to T.U. to spend a sabbatical at the Otto-von-Guericke-Universität Magdeburg.

[1] R. Diestel, *Graphentheorie* (Springer, Berlin, 1996).
[2] S. Boccaletti, V. Latora, Y. Moreno, M. Chavez, and D.-U. Hwang, Phys. Rep. **424**, 175 (2006).
[3] R. Albert and A.-L. Barabási, Rev. Mod. Phys. **74**, 47 (2002).
[4] D. J. Watts and S. H. Strogatz, Nature (London) **393**, 440 (1998).
[5] A. Barrat, M. Barthélemy, R. Pastor-Satorras, and A. Vespignani, Proc. Natl. Acad. Sci. U.S.A. **101**, 3747 (2004).
[6] R. Guimerà, S. Mossa, A. Turtschi, and L. A. N. Amaral, Proc. Natl. Acad. Sci. U.S.A. **102**, 7794 (2005).
[7] W. Li and X. Cai, Physica A **382**, 693 (2007).
[8] A. Doménech, Physica A **388**, 4658 (2009).
[9] J. R. Less, T. C. Skalak, E. M. Sevick, and R. K. Jain, Cancer Res. **51**, 265 (1991).
[10] J. Buhl, J. Gautrais, R. V. Solé, P. Kuntz, S. Valverde, J. L. Deneubourg, and G. Theraulaz, Eur. Phys. J. B **42**, 123 (2004).
[11] J. Buhl, J. Gautrais, J. L. Deneubourg, P. Kuntz, and G. Theraulaz, J. Theor. Biol. **243**, 287 (2006).
[12] A. L. Barabási, H. Jeong, Z. Néda, E. Ravasz, A. Schubert, and T. Vicsek, Physica A **311**, 590 (2002).
[13] G. Fagiolo, J. Reyes, and S. Schiavo, Phys. Rev. E **79**, 036115 (2009).
[14] I. Rodríguez-Iturbe and A. Rinaldo, *Fractal River Bassins: Chance and Self-Organization* (Cambridge University Press, Cambridge, England, 2001).
[15] C. Villani, *Topics in Optimal Transportation* (American Mathematical Society, Providence, 2003).
[16] A. Maritan, F. Colaiori, A. Flammini, M. Ciepak, and J. R. Banavar, Science **272**, 984 (1996).
[17] E. Katifori, G. J. Szöllösi, and M. O. Magnasco, Phys. Rev. Lett. **104**, 048704 (2010).
[18] F. Corson, Phys. Rev. Lett. **104**, 048703 (2010).
[19] C. J. Alexopoulos and C. W. Mims, *Introductory Mycology* (Wiley and Sons, New York, 1979).
[20] N. Kamiya, *Protoplasmic Streaming. Protoplasmatlogia* (Springer, Vienna, 1959).
[21] T. Ueda, in *Networks of Interacting Machines*, edited by D. Armbruster, K. Kaneko, and A. S. Mikhailov (World Scientific, New Jersey, 2005), p. 221.
[22] A. Adamatzky and J. Jones, J. Bionic Eng. **5**, 348 (2008).
[23] A. Tero, S. Takagi, T. Saigusa, K. Ito, D. P. Bebber, M. D. Fricker, K. Yumiki, R. Kobayashi, and T. Nakagaki, Science **327**, 439 (2010).
[24] T. Nakagaki, H. Yamada, and Á. Tóth, Nature (London) **407**, 470 (2000).
[25] T. Nakagaki, H. Yamada, and Á. Tóth, Biophys. Chem. **92**, 47 (2001).
[26] T. Nakagaki, R. Kobayashi, Y. Nishiura, and T. Ueda, Proc. R. Soc. London, Ser. B **271**, 2305 (2004).
[27] T. Nakagaki, M. Iima, T. Ueda, Y. Nishiura, T. Saigusa, A. Tero, R. Kobayashi, and K. Showalter, Phys. Rev. Lett. **99**, 068104 (2007).
[28] W. Naib-Majani, M. Osborn, K. Weber, K.-E. Wohlfarth-Bottermann, H. Hinssen, and W. Stockem, J. Cell. Sci. **60**, 13 (1983).
[29] Y. Kagawa and A. Takamatsu, Phys. Rev. E **79**, 046216 (2009).
[30] T. Akitaya, S. Ohsaka, T. Ueda, and Y. Kobatake, J. Gen. Microbiol. **131**, 195 (1985).
[31] W. Baumgarten and M. J. B. Hauser, J. Comp. Interdiscip. Sci. **1**, 241 (2010).